ELSEVIER

Journal of Organometallic Chemistry 564 (1998) 249–256

Journal of Organometallic Chemistry

The synthesis of $[AuCo(CO)_4]_2(\mu$-dppfe) (dppfe = 1,1′-bis(diphenyl phosphino)ferrocene) and the P–Au–Co–CO(axial) skeletal pair formation between neighboring molecules in the crystal

Satoru Onaka [a,*], Yoshitaka Katsukawa [b], Masahiro Yamashita [b]

[a] *Department of Environmental Technology, Graduate School of Engineering, Nagoya Institute of Technology, Gokiso-cho, Showa-ku, Nagoya 466-8555, Japan*

[b] *Division of Informatics for Science, Graduate School of Human Informatics and PRESTO(JST), Nagoya University, Chikusaku, Nagoya 464-8601, Japan*

Received 1 April 1998

Abstract

The title compound has been synthesized by reacting $(AuCl)_2(\mu$-dppfe) with $LiCo_3(CO)_{10}$ in THF at room temperature. The IR spectrum of this product in the ν(CO) region has shown that each of the three peaks observed for a solution sample splits into a doublet in the solid. Single crystal X-ray analysis has revealed that the P–Au–Co–CO(axial) skeleton makes a pair in a head-to-tail manner with neighboring molecules. The Au–Au separation in the pair is 5.6220(8) Å, which is far beyond the regime of the normal aurophilic interaction. By comparing the results with those of analogous Mn compound, that is, $[AuMn(CO)_5]_2(\mu$-dppfe), it has been concluded that the pair formation between the neighboring molecules is responsible for ν(CO) splitting of $[AuCo(CO)_4]_2(\mu$-dppfe). © 1998 Elsevier Science S.A. All rights reserved.

Keywords: Au-transition metal bond; Au···Au interaction; IR(ν(CO)) splitting; Single crystal X-ray analysis

1. Introduction

The construction of higher-nuclearity clusters and extended solid state structures with well defined dimensions from small clusters or molecular components finds the potential for novel electronic, magnetic and/or optical properties relevant to applications to nanotechnology [1,2]. We have reported the synthesis of larger metal clusters with a nanometer scale dimension from $-CCo_3(CO)_9$ clusters by the technique of the molecular design and found a strong interaction between two $-CCo_3(CO)_9$ units in p-$[(OC)_9Co_3C]_2C_6H_4$ [3]. Self-assembly techniques are also an effective means to construct such supra clusters. We have been interested in the use of aurophilic interaction (Au···Au interaction) as one of such techniques to create a more extended solid state cluster structure [4]. Therefore, we were tempted to react $LiCo_3(CO)_{10}$ with $(ClAu)_2$dppfe (dppfe = 1,1′-bis(diphenylphosphino)ferrocene) with the hope of the synthesis of $[Au\text{-}CCo_3(CO)_9]_2(\mu$-dppfe) and with the expectation that this cluster should produce an extended solid state structure through an Au-Au contact. Here we report the synthetic result, unusual ν(CO) splitting in solid states, and single crystal X-ray analysis of the product together with the single crystal X-ray analysis of analogous $[AuMn(CO)_5]_2(\mu$-dppfe).

* Corresponding author. Fax: 81 52 7355760; e-mail: onklustr@ks.kyy.nitech.ac.jp

0022-328X/98/$19.00 © 1998 Elsevier Science S.A. All rights reserved.
PII S0022-328X(98)00691-3

2. Experimental sectiony

2.1. General comments

All reactions were carried out under an argon atmosphere by standard Schlenk techniques. $(AuCl)_2(\mu$-dppfe) was prepared as previously reported [5]. $[AuMn(CO)_5]_2(\mu$-dppfe) was synthesized by the literature method [6]. ^{1}H- and ^{31}P-NMR spectra were recorded on a Varian XL-200 spectrometer; ^{31}P-NMR chemical shift is reported for H_3PO_4. IR spectra were recorded on a JASCO Valor-III FT-IR spectrometer.

2.2. Synthesis of $[AuCo(CO)_4]_2(\mu$-dppfe)(1)

An ether solution (40 ml) of $LiCo_3(CO)_{10}$ generated in situ from $Co_2(CO)_8$ (0.420 g, 1.23 mmol) was reacted with a THF solution (40 ml) of $(AuCl)_2(\mu$-dppfe) (275 mg, 0.27 mmol) at room temperature and the mixture was stirred at room temperature for 21 h. Then the solvent was vacuum-stripped and the resulting yellow solid was extracted with toluene. The yellow product was recrystallized from CH_2Cl_2: hexane (1:1) to yield 75 mg of orange yellow single crystals (yield 22% in a form of single crystals). 200 MHz ^{1}H-NMR ($CDCl_3$, 298 K): 4.24 (d, 4H, Cp), 4.82 (d, 4H, Cp), 7.42–7.52 (m, 20H, Ph). 80.984 MHz ^{31}P-NMR ($CDCl_3$, 298 K): 32.36 (s). ν(CO) (KBr disk): 2054 (s), 2049(s), 1983 (s,sh), 1975 (s), 1950 (vs), 1927 (vs) cm^{-1}. ν(CO) (CH_2Cl_2): 2054 (s) (A_1^2), 1983 (s) (A_1^1), 1951 (vs) (E) cm^{-1}. The IR spectra are shown in Fig. 1.

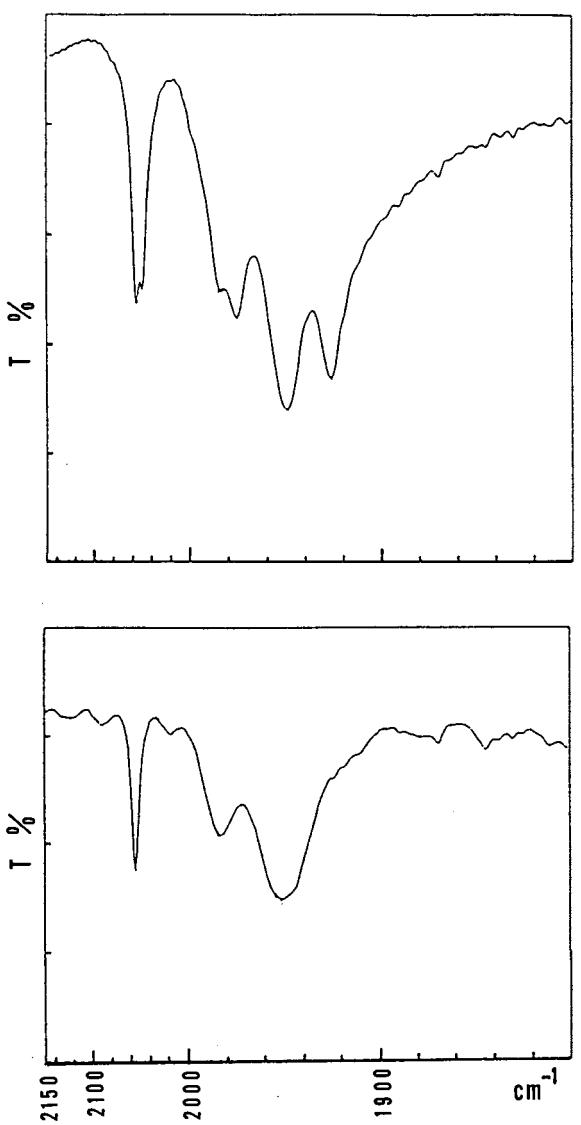

Fig. 1. IR(ν(CO)) spectra of **1**; a KBr disk sample (top) and a CH_2Cl_2 solution sample (bottom).

Table 1
Crystal data

Compound	$[AuCo(CO)_4]_2$ (μ-dppfe)(**1**)	$[AuMn(CO)_5]_2$ (μ-dppfe)(**2**)
Formula	$C_{42}H_{28}Au_2Co_2FeO_8P_2$	$C_{44}H_{28}Au_2FeMn_2O_{10}P_2$
Formula weight	1290.2	1338.3
Crystal system	Triclinic	Monoclinic
Space group	$P\bar{1}$	$A2/a$
a (Å)	12.947(3)	24.049(4)
b (Å)	16.326(8)	21.282(3)
c (Å)	10.201(4)	19.848(4)
α (deg)	95.18(4)	90
β (deg)	92.98(3)	107.16(1)
χ (deg)	107.27(3)	90
V (Å^3)	2072(2)	9706(3)
Z	2	8
$d_{calc.}$ (g cm^{-3})	2.098	1.832
Crystal dimensions (mm^3)	$0.4\times0.2\times0.1$	$0.6\times0.5\times0.35$
μ(Mo–K$_a$) (cm^{-1})	41.42	39.10
Scan type	$\omega-2\theta$	$\omega-2\theta$
Scan range	1.83 $+0.35\tan\theta$	1.45 $+0.35\tan\theta$
Scan speed (deg. min^{-1})	8.0	6.0
$2\theta_{max}$ (deg)	50.0	45.0
Temperature (K)	173	298
Unique reflections	7231	6364
Reflections with $\|F_o\| > 3\sigma(\|F_o\|)$	6168	3347
No. of parameters refined	515	550
R	0.0525	0.0959
R_w	0.0689	0.131

Mo–K$_a$ radiation ($\lambda = 0.71073$ Å); $R = \Sigma\|\|F_o\|-\|F_c\|\|/\|F_o\|$; $R_w = [\Sigma(\|F_o\|-\|F_c\|)^2/\Sigma\, w(F_o)^2]^{1/2}$ where $w = 1/\sigma^2(F)$.

2.3. Crystal structure determination

Yellow single crystals of **1** were grown from CH_2Cl_2: hexane (1:1). A crystal with approximate dimensions of $0.4\times0.2\times0.1$ was mounted on a MAC MXC^{18} diffractometer equipped with graphite monochromated Mo–

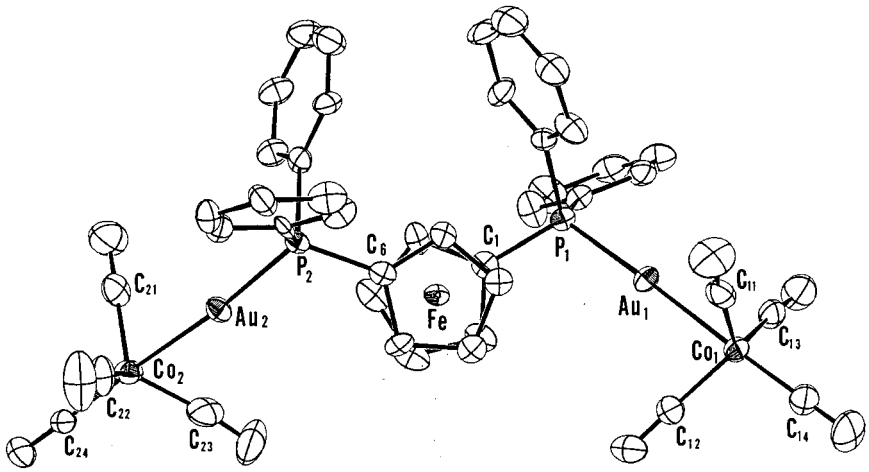

Fig. 2. The molecular structure of $[AuCo(CO)_4]_2(\mu$-dppfe)(**1**).

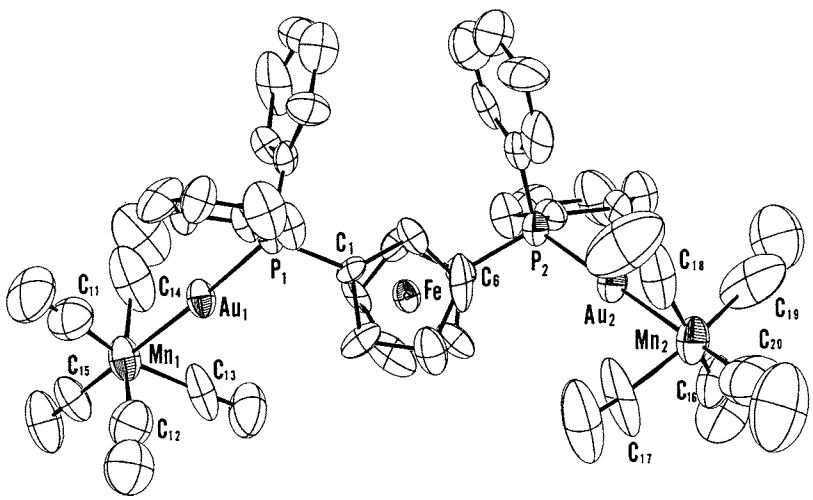

Fig. 3. The molecular structure of $[AuMn(CO)_5]_2(\mu$-dppfe)(**2**).

K_α radiation ($\lambda = 0.71073$ Å). Diffraction data were collected at 173 K. For $[AuMn(CO)_5]_2(\mu$-dppfe)(**2**), yellow single crystals were grown from CH_2Cl_2: hexane (1:1). A crystal with approximate dimensions of $0.6 \times 0.5 \times 0.35$ was sealed in a glass capillary under N_2 and was mounted on a MAC MXC[3] diffractometer equipped with graphite monochromated Mo–K_α radiation ($\lambda = 0.71073$ Å). Diffraction data were collected at 298 K. The crystal data for **1** and **2** are given in Table 1. The structures were solved by direct methods; **1** by SHELXS86 in a Crystan program package and **2** by Sir 92 in a Crystan-G program package provided by MAC Science. All non-hydrogen atoms were refined with anisotropic thermal parameters. The rather high R value for **2** was supposed at first to result from a possible disorder. However, careful inspection of the results did not support the disorder. Instead, it has been shown that the intensities of reflections are generally weak. Therefore, we rather suggest that the poor quality of the crystal is responsible for this high R value. The molecular structures of **1** and **2** are shown in Figs. 2 and 3, respectively. The atomic coordinates are listed in Table 2 and selected bond lengths and angles are given in Table 3. The $|F_o| - |F_c|$ tables and anisotropic temperature factor tables are available from the author.

3. Results and discussion

Our first purport is the synthesis of $[AuCCo_3(CO)_9]_2(\mu$-dppfe) as is described in the introductory section. The IR spectra in ν(CO) region for solid samples seemed at first glance to be an enticing evidence for harvesting such a cluster from the reaction of $(AuCl)_2(\mu$-dppfe) with $LiCo_3(CO)_{10}$, because six peaks were observed for KBr disk and/or Nujol mull samples (Fig. 1). However, single crystal X-ray analysis has shown that the product is $[AuCo(CO)_4]_2(\mu$-dppfe)(**1**) (Fig. 2). The IR spectrum for solid samples of **1** is best interpreted in terms of the splitting of each of the three peaks observed for a solution sample of **1** and this splitting is caused by a peculiar pair formation between

Table 2
Atomic coordinates and isotropic thermal parameters, B_{eq} (Å^2) for **1** and U_{eq} (Å^2) for **2**

Atom	x	y	z	B_{eq}
1				
Au1	−0.04008 (3)	0.06088 (2)	0.25928 (4)	2.15 (1)
Au2	−0.26289 (3)	0.48419 (2)	0.56673 (4)	2.17 (1)
Fe1	−0.1494 (1)	0.26874 (8)	0.4122 (1)	1.71 (3)
Co1	0.1532 (1)	0.06187 (9)	0.2566 (1)	2.21 (4)
Co2	−0.3257 (1)	0.51516 (9)	0.7873 (1)	2.54 (4)
P1	−0.2130 (2)	0.0635 (2)	0.2690 (2)	1.86 (6)
P2	−0.2269 (2)	0.4476 (2)	0.3587 (2)	1.75 (6)
C 1	−0.2245 (8)	0.1395 (6)	0.4005 (9)	2.0 (2)
C 2	−0.1496 (9)	0.1676 (6)	0.516 (1)	2.5 (3)
C 3	−0.182 (1)	0.2304 (6)	0.598 (1)	3.0 (3)
C 4	−0.2761 (9)	0.2424 (7)	0.532 (1)	2.7 (3)
C 5	−0.3033 (8)	0.1874 (6)	0.409 (1)	2.2 (2)
C 6	−0.1342 (7)	0.3846 (5)	0.3473 (9)	1.9 (2)
C 7	−0.1275 (8)	0.3247 (6)	0.2402 (9)	2.0 (2)
C 8	−0.0368 (8)	0.2943 (6)	0.272 (1)	2.0 (2)
C 9	0.0121 (8)	0.3350 (6)	0.400 (1)	2.4 (3)
C 10	−0.0488 (7)	0.3915 (6)	0.448 (1)	2.0 (2)
C 11	0.1476 (9)	0.1216 (7)	0.122 (1)	3.0 (3)
C 12	0.1554 (9)	0.1214 (8)	0.412 (1)	3.4 (3)
C 13	0.0735 (8)	−0.0472 (6)	0.236 (1)	2.8 (3)
C 14	0.2874 (9)	0.0529 (7)	0.258 (1)	3.2 (3)
C 21	−0.4546 (9)	0.4662 (7)	0.698 (1)	3.0 (3)
C 22	−0.261 (1)	0.6188 (8)	0.741 (1)	3.7 (4)
C 23	−0.250 (1)	0.4418 (9)	0.816 (1)	3.9 (4)
C 24	−0.3595 (8)	0.5464 (8)	0.949 (1)	3.0 (3)
O 11	0.1454 (8)	0.1599 (7)	0.0332 (9)	5.5 (3)
O 12	0.1595 (8)	0.1615 (8)	0.509 (1)	6.2 (4)
O 13	0.0274 (7)	−0.1199 (6)	0.221 (1)	4.2 (3)
O 14	0.3743 (7)	0.0480 (6)	0.255 (1)	5.5 (3)
O 21	−0.5392 (7)	0.4318 (7)	0.645 (1)	5.0 (3)
O 22	−0.221 (8)	0.6885 (6)	0.721 (1)	6.4 (4)
O 23	−0.199 (1)	0.3986 (8)	0.844 (1)	7.3 (4)
O 24	−0.3811 (7)	0.5683 (6)	1.0490 (8)	4.5 (3)
C 31	−0.2715 (8)	0.0932 (6)	0.1220 (9)	1.9 (2)
C 32	−0.201 (1)	0.1292 (7)	0.028 (1)	3.2 (3)
C 33	−0.242 (1)	0.1602 (8)	−0.080 (1)	3.7 (4)
C 34	−0.354 (1)	0.1504 (8)	−0.096 (1)	4.4 (4)
C 35	−0.422 (1)	0.1129 (8)	−0.007 (1)	4.0 (4)
C 36	−0.3823 (9)	0.0833 (7)	0.106 (1)	2.8 (3)
C 41	−0.3060 (7)	−0.398 (6)	0.298 (1)	1.9 (2)
C 42	−0.3783 (9)	−0.0472 (7)	0.396 (1)	3.2 (3)
C 43	−0.445 (1)	−0.1276 (8)	0.418 (1)	4.0 (4)
C 44	−0.4387 (9)	−0.2016 (7)	0.342 (1)	3.2 (3)
C 45	−0.3673 (9)	−0.1950 (7)	0.246 (1)	2.9 (3)
C 46	−0.2997 (8)	−0.1139 (6)	0.226 (1)	2.6 (3)
C 51	−0.3492 (8)	0.3816 (6)	0.262 (1)	2.1 (2)
C 52	−0.3577 (9)	0.3721 (7)	0.125 (1)	2.7 (3)
C 53	−0.453 (1)	0.3198 (8)	0.055 (1)	3.6 (3)
C 54	−0.5409 (9)	0.2737 (8)	0.120 (1)	3.8 (3)
C 55	−0.5331 (9)	0.2847 (8)	0.258 (1)	3.4 (3)
C 56	−0.4386 (8)	0.3398 (6)	0.327 (1)	2.8 (3)
C 61	−0.1675 (7)	0.5385 (6)	0.2681 (9)	1.7 (2)
C 62	−0.1002 (9)	0.5307 (7)	0.168 (1)	3.0 (3)
C 63	−0.059 (1)	0.6013 (8)	0.094 (1)	3.6 (3)
C 64	−0.0814 (9)	0.6777 (7)	0.125 (1)	3.2 (3)
C 65	−0.1464 (9)	0.6861 (7)	0.227 (1)	2.8 (3)
C 66	−0.1916 (8)	0.6147 (7)	0.298 (1)	2.6 (3)

Table 2 (Continued)

Atom	x	y	z	U_{eq}
2				
Au1	0.297 (3)	0.1454 (3)	−0.0666 (4)	0.050 (4)
Au2	−0.1532 (4)	−0.1409 (4)	−0.3552 (4)	0.055 (5)
Fe1	−0.063 (1)	−0.001 (1)	−0.205 (1)	0.04 (1)
Mn1	−0.011 (1)	0.252 (1)	−0.045 (2)	0.07 (2)
Mn2	−0.191 (2)	−0.246 (1)	−0.322 (2)	0.07 (2)
P 1	0.066 (2)	0.054 (2)	−0.097 (2)	0.04 (2)
P 2	−0.111 (2)	−0.050 (2)	−0.376 (2)	0.04 (3)
C 1	0.013 (11)	−0.007 (10)	−0.128 (13)	0.1 (2)
C 2	0.008 (16)	−0.055 (13)	−0.182 (15)	0.1 (2)
C 3	−0.040 (17)	−0.094 (11)	−0.184 (12)	0.1 (2)
C 4	−0.071 (7)	−0.069 (8)	−0.132 (10)	0.1 (1)
C 5	−0.036 (9)	−0.014 (9)	−0.097 (10)	0.1 (1)
C 6	−0.106 (13)	0.006 (10)	−0.307 (12)	0.1 (2)
C 7	−0.146 (8)	0.010 (10)	−0.266 (12)	0.1 (1)
C 8	−0.131 (9)	0.064 (9)	−0.225 (10)	0.1 (2)
C 9	−0.081 (9)	0.092 (7)	−0.238 (9)	0.1 (1)
C 10	−0.062 (10)	0.057 (9)	−0.285 (10)	0.1 (1)
C 11	0.064 (8)	0.256 (8)	0.010 (8)	0.1 (1)
C 12	−0.033 (11)	0.217 (12)	0.022 (9)	0.1 (2)
C 13	−0.081 (9)	0.217 (7)	−0.100 (8)	0.1 (1)
C 14	0.016 (12)	0.273 (12)	−0.124 (9)	0.1 (2)
C 15	−0.042 (10)	0.330 (10)	−0.036 (10)	0.1 (1)
C 16	−0.258 (13)	−0.218 (10)	−0.364 (10)	0.1 (2)
C 17	−0.191 (10)	−0.199 (10)	−0.238 (12)	0.2 (1)
C 18	−0.108 (10)	−0.259 (8)	−0.290 (9)	0.1 (1)
C 19	−0.190 (7)	−0.275 (9)	−0.409 (9)	0.1 (1)
C 20	−0.216 (9)	−0.328 (13)	−0.295 (11)	0.2 (2)
O 11	0.112 (9)	0.264 (12)	0.047 (1)	0.1 (2)
O 12	−0.039 (9)	0.192 (16)	0.079 (12)	0.1 (2)
O 13	−0.120 (7)	0.194 (8)	−0.132 (9)	0.1 (1)
O 14	0.026 (7)	0.285 (8)	−0.175 (8)	0.1 (1)
O 15	−0.062 (11)	0.376 (9)	−0.035 (11)	0.1 (2)
O 16	−0.305 (8)	−0.192 (8)	−0.390 (10)	0.1 (1)
O 17	−0.184 (9)	−0.178 (9)	−0.194 (10)	0.2 (1)
O 18	−0.058 (13)	−0.257 (10)	−0.260 (12)	0.2 (2)
O 19	−0.185 (10)	−0.279 (11)	−0.465 (12)	0.1 (1)
O 20	−0.225 (7)	−0.373 (7)	−0.266 (8)	0.27 (9)
C 21	0.125 (12)	0.020 (12)	−0.028 (15)	0.1 (2)
C 22	0.163 (10)	0.058 (11)	0.015 (12)	0.1 (2)
C 23	0.212 (6)	0.034 (8)	0.071 (8)	0.09 (9)
C 24	0.216 (11)	−0.024 (15)	0.080 (16)	0.1 (3)
C 25	0.177 (9)	−0.067 (9)	0.038 (8)	0.1 (1)
C 26	0.128 (12)	−0.045 (19)	−0.014 (16)	0.1 (3)
C 31	0.094 (11)	0.063 (12)	−0.173 (13)	0.1 (2)
C 32	0.136 (16)	0.019 (27)	−0.182 (21)	0.1 (4)
C 33	0.159 (9)	0.026 (8)	−0.238 (8)	0.1 (1)
C 34	0.145 (11)	0.078 (7)	−0.281 (11)	0.1 (1)
C 35	0.108 (18)	0.125 (12)	−0.269 (21)	0.1 (3)
C 36	0.083 (18)	0.115 (13)	−0.213 (11)	0.1 (2)
C 41	−0.038 (14)	−0.060 (11)	−0.380 (10)	0.1 (2)
C 42	−0.008 (8)	−0.020 (8)	−0.405 (8)	0.1 (1)
C 43	0.052 (12)	−0.030 (11)	−0.403 (14)	0.1 (2)
C 44	0.079 (8)	−0.087 (8)	−0.377 (8)	0.1 (1)
C 45	0.055 (14)	−0.130 (16)	−0.349 (13)	0.1 (2)
C 46	−0.007 (7)	−0.117 (9)	−0.351 (8)	0.1 (1)
C 51	−0.149 (9)	−0.007 (8)	−0.458 (9)	0.1 (1)
C 52	−0.180 (10)	−0.047 (10)	−0.513 (11)	0.1 (1)
C 53	−0.210 (7)	−0.024 (8)	−0.581 (8)	0.1 (1)
C 54	−0.216 (11)	0.038 (10)	−0.588 (12)	0.1 (1)
C 55	−0.183 (11)	0.079 (8)	−0.527 (9)	0.1 (1)
C 56	−0.151 (10)	0.055 (11)	−0.463 (16)	0.1 (2)

neighboring molecules in the solid state as is discussed later in detail. We have been interested in the solid structure (the crystal packing) of the manganese analogue, $[AuMn(CO)_5]_2(\mu$-dppfe)(**2**), in order to shed light on the solid state effect of **1** on the splitting of the ν(CO) peaks by comparing the crystal packings of **1** and **2**, as **2** is expected to have a similar molecular structure to that of **1**. Thus single crystal X-ray structure analysis of **2** is essential and has been made in the present study; the synthesis of which has previously been reported by Hor et al. without the result of X-ray analysis [6]. Although the *R* value is rather high, the structural parameters obtained are enough for our purpose. The conformation about the central Fe atom is quite similar to each other for **1** and **2** (Fig.3). The Au–Co bond lengths are 2.499(1) and 2.492(1) Å, which are slightly shorter than that of $PPh_3Au–Co(CO)_4$ (2.50(1) Å) [7] and longer than that of $Au_6(PPh_3)_4[Co(CO)_4]_2$ (2.46 Å) [8]. The Au–Mn bond lengths are 2.56(3) and 2.58(3) Å, which are consistent with that in $PPh_3Au–Mn(CO)_4\{P(OPh)_3\}$ (2.57(1) Å) [9] and are slightly longer than that of $PPh_3Au–Mn(CO)_5$ (2.52(3) Å) [10] and shorter than those of $[AuMn_2(CO)_8(\mu$-$PPh_2)]_2(\mu$-dppfe) (2.660(1) and 2.776(1) Å) [11]. Au–P bond lengths are 2.258(3) and 2.262(2) Å for **1** and 2.28(5) and 2.27(5) Å for **2,** respectively. Subtle changes in Au–P distances for these two compounds may reflect the difference in basicities of $Co(CO)_4$ and $Mn(CO)_5$. The P–Au–M backbones are almost linear (P1–Au1–Co1 = 177.78(7), P2–Au2–Co2 = 173.16(6) ° for **1** and P1–Au1–Mn1 = 174(1), P2–Au2–Mn2 = 174(2) ° for **2**, respectively). Especial linear geometry of the P1–Au1–Co1 backbone may be resulted from the pair formation in a head-to-tail manner with neighboring molecules in the crystal as is described below. Co–CO bond lengths (average 1.773 Å) in the $Co(1)(CO)_4$ group bonded to Au1 are only slightly shorter than those of the $Co(2)(CO)_4$ group (average 1.785 Å) bonded to Au2. Mn–CO bond lengths are in the range of normal bond lengths for manganese carbonyl derivatives.

Fig. 4 shows a drawing of the crystal packing of **1** along the *c*-axis; two half moieties of the neighboring molecules of **1,** especially P–Au–Co–CO (axial) skeletons are parallel and make a pair in a head-to-tail manner as if an inversion center exists in the midst of the Au1···Au1 connection. Therefore, two $Co(CO)_4$ groups in neighboring molecules of **1** are located in close proximity; the closest contact among the CO groups in the pair is 3.73(1) Å (O12···O13). The Au–Au separation is 5.6220(8) Å (Au1–Au1) (broken line in Fig. 4). The pairs are also parallel to the a axis. An a axis projection (Fig. 5) shows that the remaining half moieties of the neighboring molecules are also parallel for each other and make a pair. Thus a kind of infinite pair structure is formed in the solid state, although the closest contact among the CO groups in the pair of the remaining half moieties is beyond the distance of a significant interaction and the Au–Au separation is 6.3997(8) Å (Au2···Au2) (dashed line in Fig. 5). These geometrical features may be reflected in the subtle change in the skeletal backbone structure, that is, the linearity of P1–Au1–Co1 and P2–Au2–Co2 skeletons.

Table 3
Selected bond lengths (Å) and angles (deg)

Compound **1**		Compound **2**	
Au1–Co1	2.499(1)	Au1–Mn1	2.56(3)
Au2–Co2	2.492(1)	Au2–Mn2	2.58(3)
Au1–P1	2.258(3)	Au1–P1	2.28(5)
Au2–P2	2.262(2)	Au2–P2	2.27(5)
Fe1–C1	2.033(8)	Fe1–C1	2.0(3)
Fe1–C2	2.04(1)	Fe1–C2	2.0(4)
Fe1–C3	2.07(1)	Fe1–C3	2.1(2)
Fe1–C4	2.06(1)	Fe1–C4	2.1(2)
Fe1–C5	2.037(9)	Fe1–C5	2.1(2)
Fe1–C6	2.02(1)	Fe1–C6	2.0(1)
Fe1–C7	2.04(1)	Fe1–C7	2.0(2)
Fe1–C8	2.07(1)	Fe1–C8	2.1(2)
Fe1–C9	2.066(9)	Fe1–C9	2.1(2)
Fe1–C10	2.028(8)	Fe1–C10	2.0(2)
Co1–C11	1.76(1)	Mn1–C11	1.8(3)
Co1–C12	1.78(1)	Mn1–C12	1.7(2)
Co1–C13	1.76(1)	Mn1–C13	1.9(2)
Co1–C14	1.79(1)	Mn1–C14	1.9(2)
Co2–C21	1.78(1)	Mn1–C15	1.8(2)
Co2–C22	1.77(1)	Mn2–C16	1.7(3)
Co2–C23	1.79(2)	Mn2–C17	2.0(2)
Co2–C24	1.80(1)	Mn2–C18	1.9(2)
C11–O11	1.15(2)	Mn2–C19	1.9(2)
C12–O12	1.13(2)	Mn2–C20	2.0(3)
C13–O13	1.15(1)	P1–C1	1.8(3)
C14–O14	1.15(2)	P2–C6	1.8(2)
C21–O21	1.15(1)	P1–C21	1.8(2)
C22–O22	1.14(2)	P1–C31	1.8(2)
C23–O23	1.14(2)	P2–C41	1.8(3)
C24–O24	1.13(1)	P2–C51	1.9(2)
P1–C1	1.79(1)		
P2–C6	1.80(1)		
P1–C31	1.81(1)		
P1–C41	1.818(9)		
P2–C51	1.808(9)		
P2–C61	1.814(9)		
P1–Au1–Co1	177.78(7)	P1–Au1–Mn1	174(1)
P2–Au2–Co2	173.16(6)	P2–Au2–Mn2	174(2)
Au1–Co1–C11	81.2(4)	Au1–Mn1–C11	77(8)
Au1–Co1–C12	78.5(4)	Au1–Mn1–C12	87(8)
Au1–Co1–C13	73.4(4)	Au1–Mn1–C13	82(8)
Au1–Co1–C14	175.0(4)	Au1–Mn1–C14	80(9)
Au2–Co2–C21	81.3(4)	Au1–Mn1–C15	176(6)
Au2–Co2–C22	76.3(4)	Au2–Mn2–C16	86(8)
Au2–Co2–C23	76.4(4)	Au2–Mn2–C17	82(9)
Au2–Co2–C24	174.4(3)	Au2–Mn2–C18	78(7)
		Au2–Mn2–C19	87(12)
		Au2–Mn2–C20	177(12)

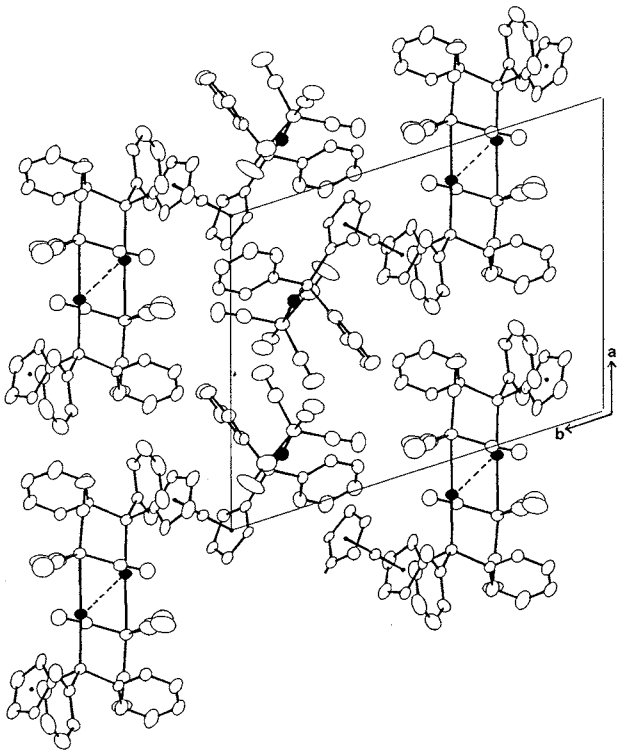

Fig. 4. A projection of the crystal of **1** along the *c*-axis.

As for **2**, the molecular packing (not shown here) is dissimilar to those of **1** in spite of the similarity of the molecular structure to **1**; no pair formation between neighboring molecules is observed in projections of the crystal structures to any direction of the unit cell, although some situations that a few CO groups in two $Mn(CO)_5$ groups of neighboring molecules look like to be located in close proximity appeared. Therefore, we are interested in the dissimilarity of ν(CO) spectra for these two compounds in solid states. Before treating solid spectra, it is better to show how the solution IR spectrum of **2** can be interpreted; **2** shows two peaks for a CH_2Cl_2 solution. The peak at 2061 cm^{-1} is assigned to the A_1^2 mode and the peak at 1955 cm^{-1} is assigned to the A_1^1 and E modes; two modes are accidentally overlapped [12–14]. Thus the overall assignment is consistent with the C_{4v} local symmetry about the Mn atom ($2A_1 + E$). Although the solid sample of **2** shows 4 peaks at 2060, 1979, 1954 and 1938 cm^{-1}, the first peak is assignable to the A_1^2, the second peak to the infrared inactive B_1, the third peak to the A_1^1, and the fourth peak to the E mode on the basis of intensity consideration [12,13]; it is not unusual that the infrared inactive B_1 mode is observed for solid samples because of the distortion from the symmetry for a free molecule [12,13]. From these analyses, it has been shown that both solution and solid spectra can be interpreted in terms of C_{4v} symmetry and the intramolecular vibrational coupling between two $-Mn(CO)_5$ groups are negligible because the intramolecular distance between these two groups are too long. In the previous papers, we and Spiro et al. have shown for $R_3M-Mn(CO)_5$ compounds that the entire IR spectra can be treated as a C_{3v} rigid group (R_3M-group) and a C_{4v} rigid group ($-Mn(CO)_5$ group) on the basis of normal coordinate treatments for all atoms [13,14]. Aforementioned conclusion on **2** is, therefore, consistent with the previous studies and each $-Mn(CO)_5$ group can be treated as an isolated single C_{4v} rigid group for both solid and solution samples. However, IR spectrum of **1** in the ν(CO) region needs some detailed analyses. A solution sample of **1** in the ν(CO) region shows three peaks at 2054, 1983, and 1951 cm^{-1} consistent with the C_{3v} local symmetry about the Co atoms ($2A_1 + E$) [12]. The peak at 2054 cm^{-1} is assigned to the A_1^2, the peak at 1983 cm^{-1} to the A_1^1, and the peak at 1951 cm^{-1} to the E mode. On the contrary, the observed IR spectra in the ν(CO) region for solid samples exhibit six peaks, suggesting the treatment described above for **2** is not applicable to **1**. In the begining we attempted to interpret the result on the basis of the molecular symmetry (C_2) for the solid sample. However, the C_2 symmetry predicts eight infrared active vibrations as a molecule. The observed spectrum for the solid sample (Fig. 1) are best interpreted in terms of the splitting of each peak under the C_{3v} point group for a solution sample as described follows; the peak at 2054 cm^{-1} (the A_1^2 mode) splits into two peaks at 2054 and 2049 cm^{-1}, the peak at 1983 cm^{-1} (the A_1^1 mode) to 1983 and 1975 cm^{-1}, and the peak at 1951 cm^{-1} (the E mode) to 1950 and 1927 cm^{-1}. We are interested in the origin of this splitting. At first we have checked the occurrence of the intramolecular coupling between two $-Co(CO)_4$ groups. However, this is not likely because the distance between two $-Co(CO)_4$ groups are too far and the splitting occurs only for solid samples. Therefore we have turned

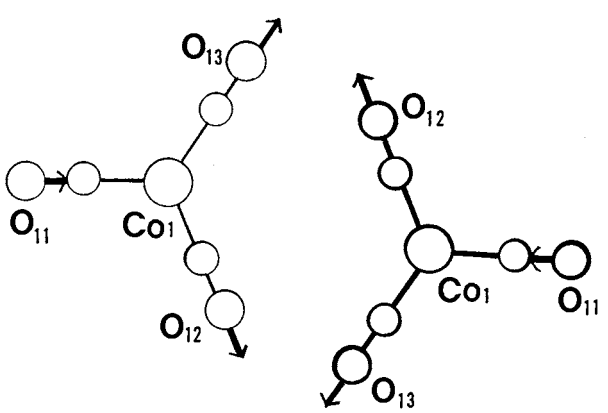

Scheme 1. Schematic representation of the dipole–dipole interaction for the E mode in the crystal of **1**. Bold circles represent an upper moiety and thin circles a lower moiety, respectively.

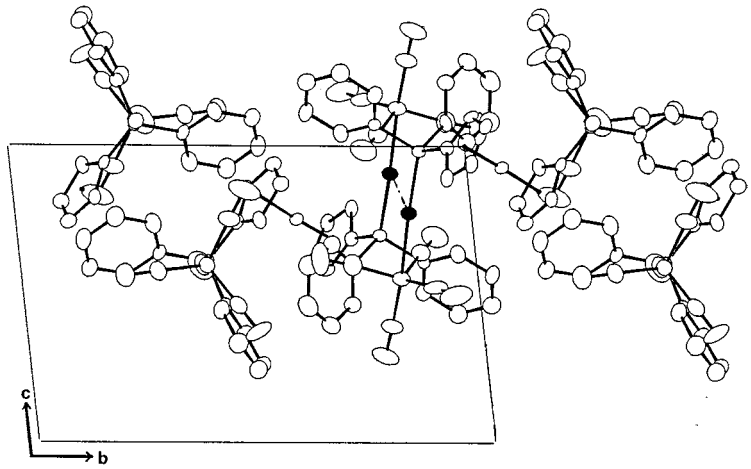

Fig. 5. A projection of the crystal of **1** along the *a*-axis.

our attention to treat the solid state spectrum on the basis of theories described in textbooks in detail [15,16]. To interplet solid state IR data, two major methods are frequently used: (1) the site symmetry approximation; and (2) the factor group and correlation field approximation [15,16]. According to many studies on the solid state IR spectra of metal carbonyl derivatives, it has now become apparent that the correlation field approximation is most effective [15–17]. However, neither the site symmetry analysis nor the correlation field analysis is applicable to the present case (**1**), because the site symmetry under the space group $P\bar{1}$ and the subgroup under the molecular symmetry (C_2) do not coincide [15]. Therefore, another approximation should be sought and we have scrutinized the solid state structures of these two compounds. The most conspicuous difference of the solid structures for **1** and **2** is that **1** composes a kind of infinite chain structure through pair formations among neighboring molecules whereas **2** does not compose such a pair structure. Therefore, it is natural for us to consider at first that the pair structure should have some responsibility for ν(CO) splitting. The splitting of these three modes in the solid is most significant for E mode as large as 23 cm^{-1} as described above. The E mode, which is a degenerate mode, is due to the vibration of the equatorial CO groups [12]. Fig. 5 (the *a*-axis projection) shows that a pair of CO groups coordinated to two $Co(1)(CO)_5$ groups are in close proximity. Scheme 1 exhibits the diagrammatic representation of the CO vibrations for the E mode within the pair in Fig. 5 as an example. The CO dipoles are in close contact with each other to make the dipole–dipole interaction in the pairs to be significant. Thus, the dipole–dipole interaction is expected to be operative for the solid state ν(CO) splitting for **1** among many possible mechanisms [15].

Next problem is to clarify why or how such pairs are formed for **1**. It is obvious that such a pair formation is not a requisite for space group symmetry. At first sight we imagined that the Au···Au interaction should have some responsibility for pair formations. However, the calculation for inter-molecular distances has shown that the Au–Au separations are 5.6220(8) Å (Au1···Au1) and 6.3997(8) Å (Au2···Au2). These distances are far beyond the regime of the aurophilic interaction (3.0–3.5 Å) [4]. At this moment, the pair formation seems to be resulted accidentally from the crystal packing force. However, we do not intend to overlook a possible role of the aurophilic interaction between the neighboring molecules for a parallel arrangement in spite of the long distance between two Au atoms. Indeed Alvarez et al. [18]. and Braunstein et al. [19]. have synthesized Au(I) complexes which possess an Au(I)-transition metal bond together with the Au···Au interaction. Thus, our effort is continuing to synthesize family compounds in which other diphosphines than dppfe are employed and clarify the crystal structures of these new compounds in order to explore a contentious role of an aurophilic interaction for this interesting pair formation.

Acknowledgements

This work was supported by Tokai Foundation for Technology and Grant-in Aids for Scientific Research No. 08874080 from the Ministry of Education, Science, Sports, and Culture, Japan. Thanks are also due to Professor M. Sano for his kind permission to use the diffractometer (MXC[18]) at low temperature.

References

[1] G. Schmid (Ed.), Clusters and Colloids—From Theory to Applications, VCH, Weinheim, 1994.

[2] L.J. de Jongh (Ed.), Physics and Chemistry of Metal Cluster Compounds, Kluwer, Dordrecht, 1994.

[3] (a) S. Onaka, M. Otsuka, A. Mizuno, S. Takagi, K. Sako, M. Otomo, Chem. Lett. (1994) 45; (b) S. Onaka, M. Otsuka, S. Takagi, K. Sako, J. Coord. Chem. 137 (1996) 151.

[4] (a) P.M. Van Calcar, M.M. Olmstead, A.L. Balch, Inorg. Chem. 36 (1997) 5231; (b) A. Bauer, H. Schmidbaur, J. Am. Chem. Soc. 118 (1996) 5324; (c) Z. Assefa, B.G. McBurnett, R. J. Staples, J.P. Fackler, Jr., Inorg. Chem. 34 (1995) 75; (d) M.J. Irwin, J.J. Vittal, G.P.A. Yap, R.J. Puddephatt, J. Am. Chem. Soc. 118 (1996) 13101 and references therein.

[5] D.T. Hill, G.R. Girard, F.L. McCabe, R.K. Johnson, P.D. Stupik, J.H. Zhang, W.M. Reiff, D.S. Eggleston, Inorg. Chem. 28 (1989) 3529.

[6] P.M.N. Low, Y.K. Yan, H.S.O. Chan, T.S.A. Hor, J. Organomet. Chem. 454 (1993) 205.

[7] T.L. Blundell, H.M. Powell, J. Chem. Soc. A (1971) 1685.

[8] J.W.A. Van Der Velden, J.J. Bour, B.F. Otterloo, W.P. Bosman, J.H. Noordik, J. Chem. Soc. Chem. Commun. (1981), 583.

[9] Kh.A.I.F.M. Mannan, Acta Crystallogr. 23 (1967) 649.

[10] H.M. Powell, K. Mannan, B.T. Kilbourn, P. Porta, Proc. Int. Conf. Coord. Chem. 8 (1964) 155.

[11] P.M.N. Low, A.L. Tan, T.S. Hor, Y.-S. Wen, L.-K. Liu, Organometallics 15 (1996) 2595.

[12] (a) L.M. Bower, M.H.B. Stiddard, J. Chem. Soc. A (1968) 706; (b) H.D. Kaesz, R. Bau, D. Hendrickson, J.M. Smith, J. Am. Chem. Soc. 89 (1967) 2844.

[13] (a) S. Onaka, Bull. Chem. Soc. Jpn. 44 (1971) 2135; (b) S. Onaka, Bull. Chem. Soc. Jpn. 46 (1973) 2444.

[14] A. Terzis, T.C. Strekas, T.G. Spiro, Inorg. Chem. 13 (1974) 1346.

[15] F.A. Cotton, Chemical Applications of Group Theory, Ch. 10, 3rd edition, Wiley, New York, 1990.

[16] K. Nakamoto, Infrared and Raman Spectra of Inorganic and Coordination Compounds, Ch. 1, 5th edition, Wiley, New York, 1997.

[17] (a) H.J. Buttery, G. Keeling, S.F.A. Kettle, I. Paul, P.J. Stamper, J. Chem. Soc. (A) (1969), 2224; (b) H.J. Buttery, G. Keeling, S.F.A. Kettle, I. Paul, P.J. Stamper, J. Chem. Soc. (A) (1970) 471; (c) H.J. Buttery, S.F.A. Kettle, G. Keeling, I. Paul, P.J. Stamper, J. Chem. Soc. Dalton Trans. (1972) 2487; (d) D.A. Kariuki, S.F.A. Kettle, Inorg. Chem. 17 (1978) 141; (e) J.S. Kristoff, D.F. Shriver, Can. J. Spectrosc. 19 (1974) 156.

[18] S. Alvarez, O. Rossell, M. Seco, J. Valls, M.A. Pellinghelli, A. Tiripicchio, Organometallics 11 (1991) 2309.

[19] P. Braunstein, M. Knorr, A. Tiripicchio, M. Tiripicchio, Inorg. Chem. 31 (1992) 3685.